Quantum Mechanics Calculations of the Thermodynamically Controlled Coverage and Structure of Alkyl Monolayers on Si(111) Surfaces

E. Joseph Nemanick, Santiago D. Solares, William A. Goddard, III,* and Nathan S. Lewis*

Division of Chemistry and Chemical Engineering, Kavli Nanoscience Institute and Beckman Institute, 127-72, Noyes Laboratory, California Institute of Technology, Pasadena, California 91125

Received: January 30, 2006; In Final Form: April 5, 2006

The heat of formation, ΔE, for silicon (111) surfaces terminated with increasing densities of the alkyl groups CH_3- (methyl), C_2H_5- (ethyl), $(CH_3)_2CH$- (isopropyl), $(CH_3)_3C$- (*tert*-butyl), $CH_3(CH_2)_5$- (hexyl), $CH_3(CH_2)_7$- (octyl), and C_6H_5- (phenyl) was calculated using quantum mechanics (QM) methods, with unalkylated sites being H-terminated. The free energy, ΔG, for the formation of both Si−C and Si−H bonds from Si−Cl model componds was also calculated using QM, with four separate Si−H formation mechanisms proposed, to give overall ΔG_S values for the formation of alkylated Si(111) surfaces through a two step chlorination/alkylation method. The data are in good agreement with measurements of the packing densities for alkylated surfaces formed through this technique, for Si−H free energies of formation, ΔG_H, corresponding to a reaction mechanism including the elimination of two H atoms and the formation of a C═C double bond in either unreacted alkyl Grignard groups or tetrahydrofuran solvent.

I. Introduction

Si(111) surfaces have been functionalized by a variety of methods, including reaction with unsaturated alkenes through a radical process catalyzed by a diacyl peroxide initiator,[1,2] use of UV[3−5] or white[6] light, thermal energy,[7,8] transition metal complexes,[9] Lewis acid catalysts,[10−12] electrochemical functionalization,[13,14] radical halogenation,[15] and transmetalation with alkyl Grignard and lithium reagents.[15−17] These surfaces have shown excellent chemical stability under a variety of conditions, and alkylation even at partial coverage of the surface Si sites greatly inhibits the oxidation of the silicon surface. In many cases, the surfaces are only partially terminated with alkyls, with proposals that nonalkylated Si sites are terminated by -OH,[2] or -H groups.[18,19] In other cases, significant oxidation of the initially alkylated surface, with the oxide present either in separate phases[20] or as mixed alkyl and Si−O−C bonding,[1] has been proposed.

Other than methyl- and ethyl-terminated surfaces prepared by a two-step chlorination/alkylation process, which have been imaged by scanning tunneling microscopy,[21,22] no direct two-dimensional structural information is available for such systems. The limiting packing density of long-chain, saturated alkyls has been claimed to be 50% of a monolayer of Si atop sites.[2,5,7] In contrast, CH_3-terminated Si(111) surfaces exhibit a 1×1 structure in low-energy electron diffraction (LEED)[18,23] and scanning tunneling microscopy (STM) experiments,[21,22] and exhibit signals in soft-X-ray spectroscopy (SXPS)[18] and infrared (IR) absorption[19,24] measurements which indicate that complete coverage of Si atop sites can be achieved. XPS data[19] and STM data[22] on ethyl-terminated Si(111) surfaces indicate that $80 \pm 10\%$ of a monolayer coverage can be attained for surfaces functionalized with ethyl groups using the chlorination/alkylation method.

The structures of alkylated Si(111) surfaces have been investigated theoretically, with previous computational studies focusing on long-chain alkyl groups, such as octyl or octadecyl groups.[25−28] In some cases, 50% coverage was assumed to be the highest packing available for such alkyl groups, and the minimum energy structure was calculated at this coverage level.[25] In other calculations, the energy per chain for octyl or octadecyl groups attached to the surface was calculated to be minimized at 40−60% alkylation of the unreconstructed Si-(111) atop sites, and minimum energy structures were calculated at the coverage that produced the minimum energy per chain.[27] For these dynamics simulations with long-chain alkyl monolayers, the van der Waals interactions of the chain tails will dominate the packing interactions. The calculated coverage that minimizes the energy per chain would predict the experimentally observed coverage only if the strain energy were the only consideration. However, the free energy change of the reaction must control the final surface coverage, and a sufficiently negative (or positive) free energy change per site reacted can cause the free energy minimum to be different from the strain energy minimum. For surfaces prepared by the chlorination/alkylation method, which has a large free energy change that favors the products relative to the reactants, higher coverages, and structures with significant bond strain, should be accessible thermodynamically, especially for functionalization reactions using very-short-chain alkyl groups, which should have less strain at higher packing densities.

Herein we report the results of quantum mechanical calculations to obtain the free energy of formation for packed alkyl groups on Si(111) at various surface coverages. The energy values have been referenced to the energy of the reactants and products of the chlorination/alkylation reaction using alkyl Grignards. This thermodynamic approach allows for the determination of the packing densities and associated structures of alkyl monolayers formed by a reaction with a large driving force, such as reaction of the Cl-terminated Si surface with a Grignard reagent. The surfaces considered represented the bulk of packed surfaces, as repeat unit cells were employed to remove any edge effects for the calculations. Linear alkyl groups investigated were $-CH_3$, $-C_2H_5$, $-C_6H_{13}$, and $-C_8H_{17}$, in addition to the bulkier groups isopropyl, *tert*-butyl, and phenyl (C_6H_5). Functionaliza-

10.1021/jp060640+ CCC: $33.50
Published on Web 07/13/2006

tion with all of these groups is experimentally accessible using the chlorination/alkylation approach.[15−20] For all calculations (except for the ethylated surface with 66.7% coverage, which required a 3 × 3 unit cell), a 2 × 2 unit cell was used with alkyl surface coverages of 25%, 50%, 75%, and 100%.

II. Methods

The relaxed geometry of all surface structures was first calculated using molecular dynamics (MD) and then refined using quantum mechanics (QM). Molecular dynamics simulations (geometry optimization, followed by 5 ps equilibration at 600 K and 15 ps at 300 K, followed by a second geometry optimization) were conducted using Cerius2 software (Accelrys, San Diego, CA), with force-field parameters previously reported for silicon[29,30] and hydrocarbons[31] (any missing parameters required for new combinations of atom types were also taken from the latter force field). Atomic charges for these simulations were obtained using the charge equilibration method (QEQ).[32] The resulting structures were then used as the initial geometry in QM calculations performed with SeqQuest software[33] within the GGA PBE[34] approximation of density functional theory (DFT). Double-ζ plus polarization basis sets and pseudopotentials were used for all atoms (see Supporting Information for a description of pseudopotentials, basis sets, K-points, wave function grids, and spin polarization settings).

Surfaces were formed from stacks of bulk crystalline silicon, with the (111) face exposed three double-layers deep and with the bottom surface terminated with hydrogen atoms. This number of bulk silicon layers resting on a fixed hydrogen layer has been shown to be an optimal compromise between accuracy and computation cost through extensive QM geometry optimization calculations on reconstructed Si(111) surfaces.[35] Periodic boundary conditions were used to avoid edge effects. The unit cell consisted of four 1 × 1 unit cells in all cases (i.e., 2 × 2), except for the 66%-ethylated surface (3 × 3), for which all atoms, except for the bottom hydrogen layer, were allowed to relax. Alkylated surfaces were constructed to be H-terminated, and alkyl groups, R-, were bound to the surface, replacing H atoms with a surface coverage of R groups of 25%, 50% 75%, or 100% (note that only one geometric arrangement of the R groups is possible for each of these coverages on the 2 × 2 unit cell), as well as 66.7% coverage for the $-C_2H_5$ terminated surface on a 3 × 3 unit cell. For the isopropyl, phenyl, and *tert*-butyl groups, calculations were also performed with two unpaired electrons, to determine if dissociation would occur due to the high steric repulsions at 75% or 100% coverage.

In each case, the average strain energy of the R groups on the surface was calculated by comparing their average bond energy on the surface unit cell to that on a hydrogen-passivated Si_{10} cluster (see Figure 1), which simulated a 1 × 1 surface site containing no nearest neighbors, and was assigned zero strain. The bond energy of the R groups to the hydrogen-passivated Si_{10} *cluster* was calculated as the difference in energy between the singlet state and the *dissociated* triplet state consisting of the radical R (containing one unpaired electron) and the hydrogen-passivated Si_{10} radical (also containing one unpaired electron) obtained after breaking the Si−R bond and separating the fragments. The average bond energy of the R groups to the *surface* was calculated in a similar fashion, except that in this case the dissociated state consists of the R radical and the surface radical (the latter is a periodic structure). The surface strain is the difference between these two values of the bond energy. When the surface contained more than one R group in the unit cell, the dissociated surface state consisted of all the dissociated R groups (containing one unpaired electron each), and the resulting surface containing one unpaired electron from the broken bond to each of the R groups.

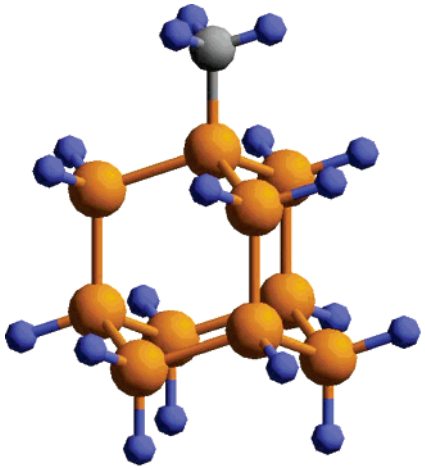

Figure 1. $Si_{10}H_{15}$ cluster simulating a 1 × 1 surface site functionalized with a methyl group, containing no nearest neighbors. Blue = hydrogen, gray = carbon, orange = silicon.

To evaluate the free energy of reaction for the formation of each alkylated surface at room temperature, $\Delta G^{298\circ}$ for the reactions:

$$\mathrm{Si(111)-Cl + CH_3MgCl \rightarrow Si(111)-CH_3 + MgCl_2} \quad -41.0 \text{ kcal/mol} \quad (1)$$

$$\mathrm{Si(111)-Cl + C_2H_5MgCl \rightarrow Si(111)-H + MgCl_2 + C_2H_4} \quad -24.2 \text{ kcal/mol} \quad (2)$$

$$\mathrm{Si(111)-Cl + C_2H_5MgCl + THF \rightarrow Si(111)-H + MgCl_2 + C_2H_6 + DHF} \quad -25.8 \text{ kcal/mol} \quad (3)$$

$$\mathrm{Si(111)-Cl + C_2H_5MgCl + THF \rightarrow Si(111)-H + MgCl_2 + (THF-C_2H_5)'} \quad -43.8 \text{ kcal/mol} \quad (4)$$

$$\mathrm{Si(111)-Cl + C_2H_5MgCl + THF \rightarrow Si(111)-H + MgCl_2 + (THF-C_2H_5)''} \quad -45.7 \text{ kcal/mol} \quad (5)$$

$$\mathrm{Si(111)-Cl + C_2H_5MgCl \rightarrow Si(111)-C_2H_5 + MgCl_2} \quad -47.1 \text{ kcal/mol} \quad (6)$$

was calculated using the Jaguar software (B3LYP flavor of DFT with 631G** basis sets) within the Poisson−Boltzmann continuum solvation model, using tetrahydrofuran (THF) as the solvent (assuming a dielectric constant of 7.52 and a solvent radius of 2.526 Å). For this calculation, the silicon site was modeled as a $Si-(SiH_3)_3$ cluster, to which either Cl, H, or R were bonded. DHF is dihydrofuran, resulting from the elimination of 2 H atoms from THF to passivate the silicon site as well as the alkyl Grignard. $(THF-C_2H_5)'$ results from bonding the alkyl group to the C atom adjacent to the O atom in THF, and $(THF-C_2H_5)''$ results from bonding to the C atom across the ring from the O atom of THF. The use of these ΔG values allows for the determination of the overall thermodynamics of these reactions over a range of possible reaction schemes.

For the determination of the free energy of formation for a surface (ΔG_S), the reaction energy for the formation of the Si−C bond for ethylation (eq 6) was used across all groups larger

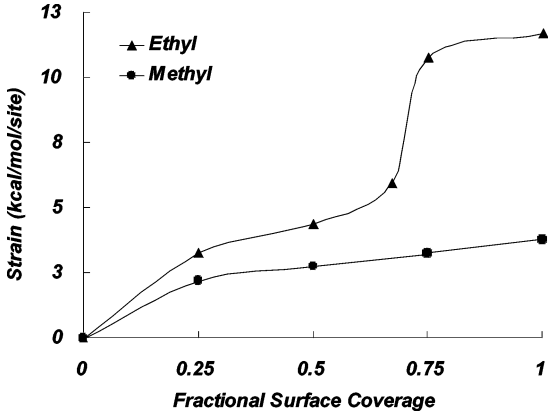

Figure 2. Strain energy per occupied surface site from quantum mechanics calculations for Si(111)−CH_3 and Si(111)−C_2H_5 as a function of surface coverage. The sites not occupied with ethyl or methyl were terminated with hydrogen atoms. The reference is an ethyl or methyl group bonded to a 1 × 1 site cluster with no nearest neighbors (see Figure 1). From ref 22.

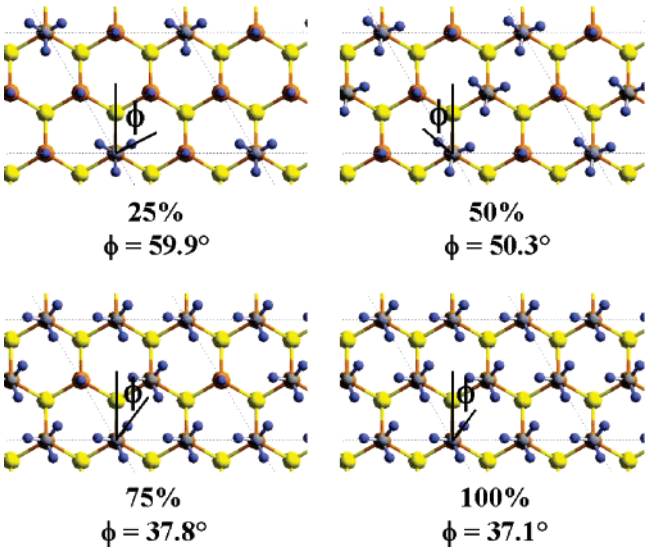

Figure 3. CH_3-terminated Si(111) surface, at 25%, 50%, 75%, and 100% coverage. The sites not occupied with methyl were terminated with hydrogen atoms. The dotted lines show the 2 × 2 unit cell used in the calculations. As the packing density θ rose, the torsion angle shifted from ~59.9° at 25% to ~37.1° at 100%. Note that the torsion angle for the structure with 50% coverage was measured *counterclockwise* from the Si−Si bond, while it was measured *clockwise* for 25%, 75%, and 100%. This is because in each case there exist two energetically equivalent structures: one in which the angle of interest (between 0° and 60°) occurs in the clockwise direction and one in which it occurs in the counterclockwise direction. In a molecular dynamics simulation, both energy minima are equally likely to occur. Blue = hydrogen, gray = carbon, orange = first layer silicon, and yellow = second layer silicon.

than methyl. ΔG_S for the formation of a particular surface of packing density, θ, was calculated by:

$$\Delta G_S = \Delta G_a \cdot \theta + \Delta G_H(1 - \theta) + \Delta E_s \qquad (7)$$

where ΔG_a is the driving force for the alkylation reaction, either −41.0 kcal/mol for CH_3-terminated surfaces or −47.1 kcal/mol for all other R groups, θ is the fraction of a unit cell alkylated (i.e. 0.75 for a 75% packed surface), ΔG_H is the ΔG for the formation of the Si−H bond, and ΔE_s is the strain energy *per* 1 × 1 unit cell for that particular coverage. Using this approach, a value for ΔG_S accompanying the production of a surface having a packing density θ can then be calculated for each possible mechanism for the production of a Si−H bond from Si−Cl. Due to the uncertainty in the mechanism for this reaction, ΔG_S curves for each surface alkylation were prepared using ΔG_H values that spanned the energy values for the mechanisms proposed, −25, −31, −38, and −45 kcal/mol. Given the likelihood that the reaction contains at least one radical-based step,[18,19] the overall formation of Si−H bonds can possibly be a combination of most or all of these steps and possibly other mechanisms not considered here, necessitating the use of a spectrum of ΔG values.

III. Results and Discussion

A. Calculated Strain Energies. Figure 2 shows the calculated strain energy for CH_3- and C_2H_5-terminated 2 × 2 surfaces at varying packing densities, θ. The CH_3-terminated surface showed a steady increase in the strain energy per molecule as θ was increased. The 2.21 kcal/mol per molecule strain energy at θ = 25% represents the overall unfavorable interaction from binding a single CH_3- group to the Si(111) surface, as the nearest -CH_3 neighboring groups were far enough removed that no strain could result from nearest-neighbor interactions. As θ increased, nearest-neighbor interactions caused an added marginal strain per bonded CH_3-, resulting in slightly higher average strain per bound molecule. The 0.56 kcal/mol energy difference between θ = 25% and θ = 50% was due to such interactions and was seen in the rotation of the -CH_3 groups from their preferred orientation atop the Si atoms of ~60°, to an angle of ~50°. Figure 3 shows the twisting of the Si−Si−C−H angle as the number of bonded -CH_3 groups increased. The -CH_3 groups at θ = 25% were staggered relative to the Si−Si bonds underneath, with the torsion angle, ϕ, calculated to be 59.9°, which represents a minimum in the torsion strain energy. When the CH_3- groups were presented with a neighbor, however, the torsion angle changed from ϕ = 59.9° to ϕ = 50.3° at θ = 50% and to ϕ = 37.8° at θ = 75%, where ϕ remained for higher densities. This twisting results from an attempt to minimize the H- - -H interactions on adjacent -CH_3 groups, as can be seen in the C−H bonds twisting to point away from the C−H bonds on adjacent Si atoms. As the packing density rose from θ = 50% to 75%, even though ϕ decreased from 50.3° to 37.8°, no significant step in strain energy per molecule was calculated, indicating that the energy minimum represented by the staggered conformation of the CH_3- groups with respect to the underlying Si−Si structure on the surface was relatively shallow in comparison to other torsion angles. The minor shift in the torsion angle as θ increased from 75% to 100% indicated that a torsion angle of $\phi \approx 37°$ presented the fewest unfavorable steric interactions for all neighbor−neighbor interactions.

The C_2H_5-bound surfaces showed a similar increase in strain energy, ΔE_s, at low packing densities from $0 \leq \theta \leq 50\%$, relative to the strain energy on the CH_3-terminated Si surface. This behavior indicates that the strain is due to -C_2H_5 group rotations into unfavorable conformations with respect to the underlying Si−Si bonds. However, a large jump in ΔE_s was observed between θ = 66.6% and θ = 75%, indicating that as the packing density increased, the strain forced bonded molecules to distort more than could be acccomplished exclusively by rotation of the alkyl groups. Figure 4 shows a side-on view of C_2H_5-terminated surfaces at θ = 66.7% and θ = 75%, demonstrating that to accommodate the larger number of groups on the surface, the ethyl group atoms must distort out of individual tetrahedral geometry to minimize steric interactions

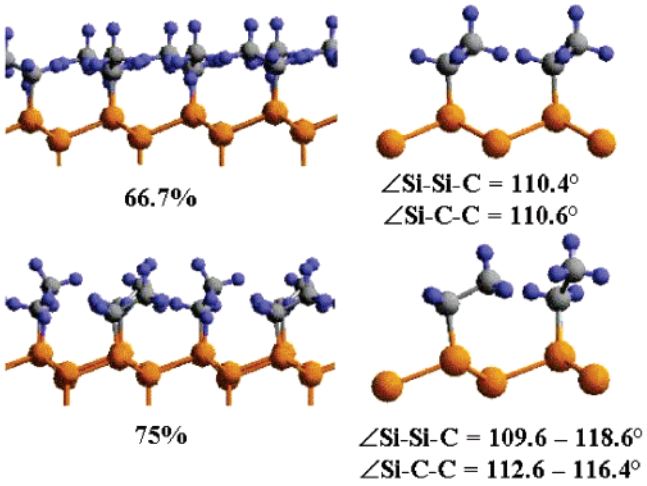

Figure 4. Side view of $-C_2H_5$ groups bonded to Si(111) at $\theta = 66.7\%$ and 75% packing density. As the packing density rose, the $-C_2H_5$ groups became more distorted, and bent vertically away from the surface to accommodate their neighbors. Blue = hydrogen, gray = carbon, orange = silicon.

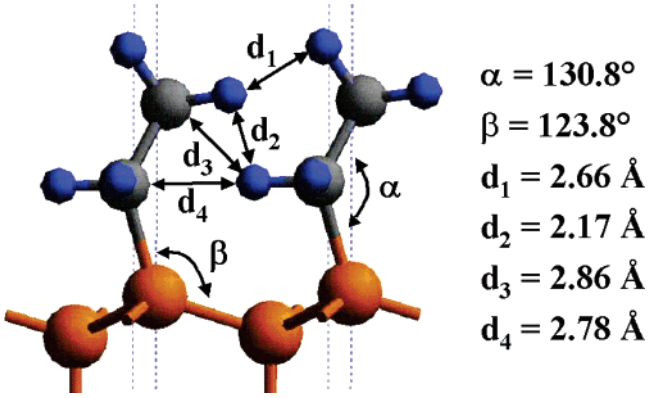

Figure 5. 100% packed C_2H_5−Si(111) surface, showing significant strain in the bond angles and nearest-neighbor nonbond distances. Blue = hydrogen, gray = carbon, orange = silicon. From ref 22.

between adjacent groups. At $\theta = 66.7\%$, the Si−C−C bond angle of 110.6° is very close to the unstrained tetrahedral angle. However, at $\theta = 75\%$, this angle increased to between 112.6 and 116.4°, and the Si−Si−C bond angle rose to between 109.6° and 118.6°, leading to the sharp jump in overall surface strain energy seen in Figure 2. After this jump, the strain energy leveled off at $\theta = 75\%$, indicating that each additional molecule added after $\theta \approx 75\%$ underwent a similar distortion to bind to the surface. Figure 5 shows the final bond angles for the $\theta =$ 100% surface, where the Si−C−C bond angle has risen to 130.8° and the Si−Si−C bond angle has risen to 123.8°, resulting in a significant portion of the 11.72 kcal/mol strain energy for each site.

Figure 6 shows the strain energy for the hexyl, octyl, isopropyl, *tert*-butyl, and phenylated surfaces as a function of the fractional coverage, θ. The surfaces evaluated to compile Figure 6 all had significantly more strain energy per molecule than either the CH_3- or C_2H_5-terminated surfaces at similar values of θ (Figure 2). Due to both the larger surface areas for unfavorable interactions from neighboring alkyl groups, and to branching in the isopropyl, *tert*-butyl, and phenyl groups, at low packing densities the distance to adjacent bonded groups decreased, resulting in more strain per bonded group relative to termination with methyl or ethyl groups. The strain energy of the two branched groups, isopropyl and *tert*-butyl, rose faster

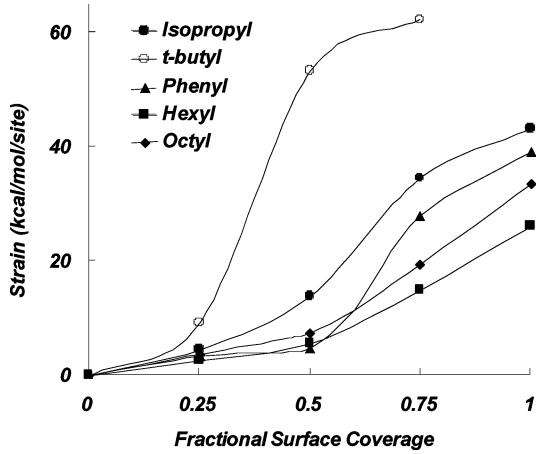

Figure 6. Calculated strain energy per occupied surface site for the alkyl groups *iso*-propyl, *tert*-butyl, phenyl, hexyl, and octyl, bonded to Si(111) surfaces at increasing packing densities. The energies of the 100% *iso*-propylated and phenylated surfaces, as well as that of the 75% *tert*-butylated surface, correspond to the triplet state (i.e. a state in which one of the functional groups has dissociated from the surface), which was significantly lower in energy than the singlet state. This indicates that these densely packed surfaces are not stable thermodynamically.

at low packing densities than for any of the other groups. At 50% packing, the phenyl-bonded surfaces, with the same degree of branching at the bonded carbon as the isopropyl group (i.e. two carbon atoms attached to the Si−C carbon), had the lowest strain energy of all groups shown in Figure 6. However, this strain energy quickly rose, and at $\theta = 75\%$ the strain energy was greater than that of the straight-chain groups. When initially presented with neighboring groups, the shorter C−C and C−H bonds of the aromatic phenyl group, as well as the more compact in-plane arrangement of the atoms, allowed phenyl to pack more efficiently by turning face-to-face. However, this beneficial arrangement was quickly lost as θ increased, due to rings in perpendicular directions being forced into unfavorable edge-on interactions (since sp^2 carbon atoms are planar and highly stiff to out-of-plane deformation). For the isopropyl and phenyl groups with $\theta = 100\%$, as well as for *tert*-butylated surfaces with $\theta = 75\%$, the average strain energies corresponded to the triplet state (i.e. a state in which one of the functional groups has dissociated from the surface). This triplet state was lower in energy than the singlet state under such conditions. This behavior indicates that these specific surfaces are not thermodynamically stable, and instead would dissociate if formed.

Figure 7 shows the conformations of hexyl and octyl groups, respectively, when bonded to the Si(111) surface. As the packing density increased, these chains bonded at increasing *tilt* angles, λ, relative to the surface. At the lowest calculated packing density, $\theta = 25\%$, hexyl and octyl groups packed with tilt angles of $\lambda = 59.9°$ and $\lambda = 57.1°$, respectively. For isolated hexyl and octyl chains on the Si(111) surface, the λ values calculated using MD (64.4° and 63.3°, respectively) were in good agreement with the λ values calculated for $\theta = 25\%$ using QM, indicating that steric interactions at $\theta = 25\%$ were negligible. As the packing density was increased in the QM calculations, λ quickly increased for both hexyl and octyl groups, with the groups being near vertical at $\theta \geq 75\%$, especially for the octyl chains. These results stand in contrast to measurement of the surface bonding angles for alkyl surfaces that were presumed to be ~50% packed when formed by hydrosilation.

In addition to the energy minimum at $\lambda = 57.1°$, the octyl-terminated surface at $\theta = 25\%$ also exhibited a local energy

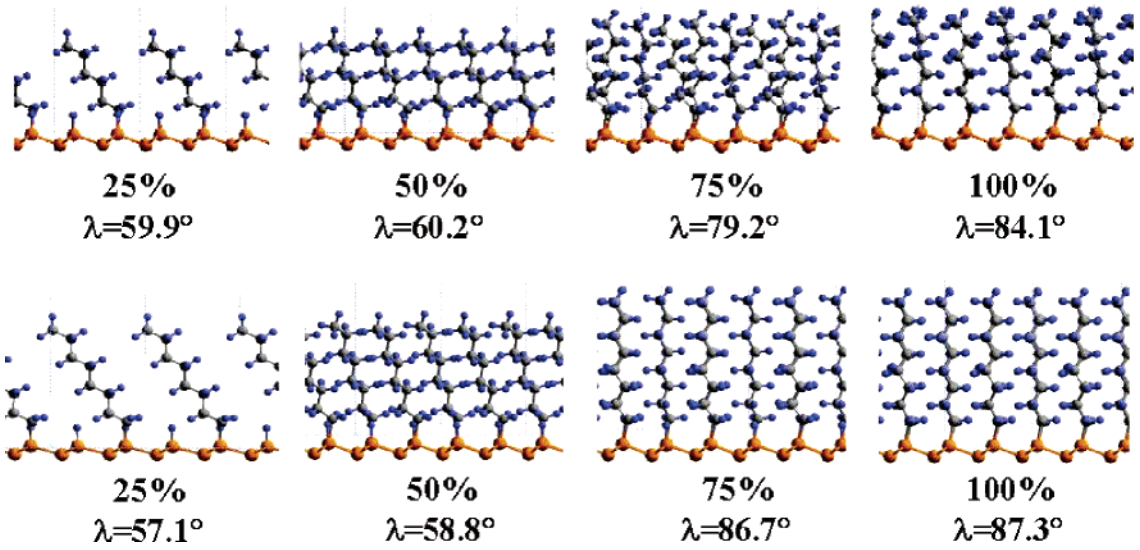

Figure 7. Side view of hexyl- and octyl-terminated Si(111) surfaces at varying packing densities, illustrating how the chain bond angle relative to the Si(111) surface, λ, increases as the packing density rises. Blue = hydrogen, gray = carbon, orange = silicon.

minimum at $\lambda = 40.5°$. This minimum was ~0.4 kcal/mol/(1 × 1 cell) higher in energy than the global minimum at this packing density. This second conformation is a consequence of the ability of the octyl chains to overlap their two terminal methylene groups with the base of neighboring chains and thereby induce a favorable van der Waals interaction that is not possible in the packing of the shorter hexyl chains. As the alkyl chain becomes longer than eight carbon atoms, these favorable van der Waals interactions are expected to increase. This observation is in agreement with the chain tilt angles obtained from surface IR dichroism measurements for the longer-chain hexadecyl groups,[2] in which $\lambda = 58°$ was deduced for surfaces prepared using heat in neat olefin, but $\lambda = 34-36°$ was deduced for samples prepared at a higher temperatures. This behavior suggests that the difference in preparation temperature caused a shift from a local minimum to the global minimum.

B. Free Energy of Formation of Alkyl Surfaces. For determination of the expected final surface packing density using these QM calculations, ΔG values are required for the surface reactions that result in the alkylation of a Si site as well as for the reactions that produce H-termination of a Si site. However, as mentioned above, several plausible reaction pathways, which have greatly varying ΔG values, could result in H-termination. Without specific data on the reaction products, the free energy for the reaction of Si−Cl to produce Si−H/R can only be bound into a range of possible ΔG values.

Figure 8 shows the free energy of formation, ΔG_S, for CH_3- (solid line) and C_2H_5-terminated (dashed line) surfaces for such a range of processes. The solid lines in Figure 8 show the free energy of formation to form an increasing fraction of CH_3-termination from a Si−Cl surface, with the four different ΔG_H values for the formation of Si−H from Si−Cl (−25, −31, −38, and −45 kcal/mol) spanning the range of ΔG_H values for the proposed reactions. For the two low driving-force energies, at all coverages methylation of a Si−Cl site was thermodynamically preferred over H-termination, as seen by steadily decreasing ΔG values as the packing density increased. As the ΔG_H for the formation of Si−H became more negative, however, at all fractional coverages, the H-termination reaction was calculated to be more thermodynamically favorable than formation of Si−C bonds. Since measurements of the surfaces formed by the two-step chlorination/alkylation reaction indicate that the surface is fully CH_3-terminated,[18,19,21] ΔG_H must either be $\lesssim -38$ kcal/mol (for which the free energy curve is nearly horizontal in Figure 8), or the reaction must have strong kinetic factors that influence the surface formation to favor alkylation over H-termination.

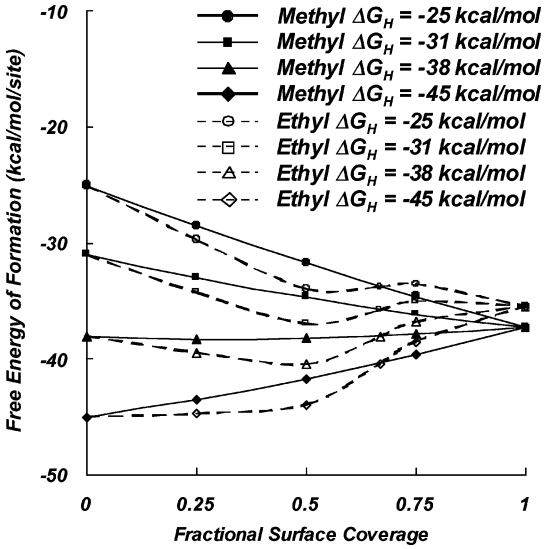

Figure 8. Free energy of formation for CH_3- (solid) and C_2H_5-terminated (dashed) Si(111) surfaces at varying fractional surface coverages, for four different ΔG_H values: −25 (circle), −31 (square), −38 (triangle), and −45 kcal/mol (diamond).

The C_2H_5-termination reaction, as seen in Figure 2, has higher strain energies associated with it, and the step in ΔE_s at $\theta \approx 66.7\%$ creates a dip around $\theta = 50\%$ across all ΔG_H values (Figure 8). The high density of C_2H_5- groups measured on these surfaces,[19,22] $\theta = 80 \pm 20\%$, also indicates that the ΔG_H for the Si−H formation is on the more positive side of the energy spectrum being considered, and that 100% coverage is not necessarily limited by thermodynamics but by high reaction barriers caused by the bulky transition states.

Figure 9 illustrates the effects of longer chains on the free energy of formation of these alkylated surfaces, showing the result of the increased strain energy. For both hexyl- and octyl-terminated surfaces for $\Delta G_H \gtrsim -43$ kcal/mol, the formation of the alkyl bond had a broad, deep minimum at $\theta \approx 50\%$. Only

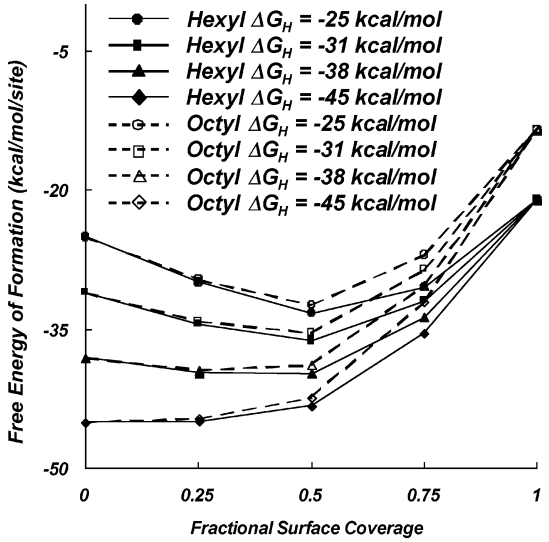

Figure 9. Free energy of formation for hexyl- (solid) and octyl-terminated (dashed) Si(111) surfaces at varying fractional surface coverages, for four different ΔG_H values: −25 (circle), −31 (square), −38 (triangle), and −45 kcal/mol (diamond).

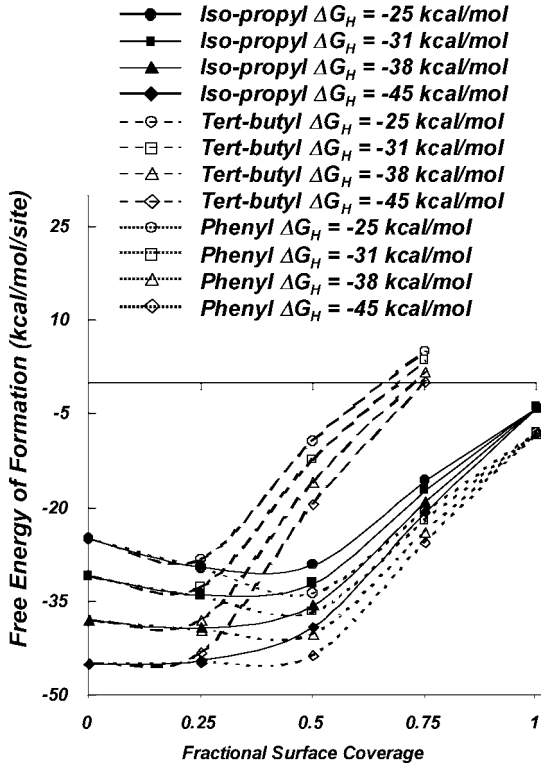

Figure 10. Free energy of formation for isopropyl- (solid), *tert*-butyl- (dashed), and phenyl-terminated (dotted) Si(111) surfaces at varying fractional surface coverages, for four different ΔG_H values: −25 (circle), −31 (square), −38 (triangle), and −45 kcal/mol (diamond). The energies of the 100% isopropylated and phenylated surfaces, as well as that of the 75% *tert*-butylated surface, correspond to the triplet state (i.e. a state in which one of the functional groups has dissociated from the surface), which was significantly lower in energy than the singlet state.

at $\Delta G_H = -45$ kcal/mol was Si−H formation favored over formation of Si−R. The minima for the octyl curves for the more positive ΔG_H values were in good agreement with experimental measurements of the coverage of octyl groups formed through the two-step reaction process.[19,22] Figure 10 shows the free energy of formation for the bulkier groups considered. The sharp divergence in ΔG_S between the isopropyl and *tert*-butyl groups highlights the large difference in the strain energy of the two groups, and leads to a lower predicted surface coverage for *tert*-butylated surfaces compared to isopropylated surfaces. The minima for both the isopropyl and *tert*-butyl surfaces lie in the region $25 \leq \theta \leq 50\%$ surface coverage for the −25 and −31 kcal/mol ΔG_H lines, with the *tert*-butyl ΔG_S rising faster as θ increases. X-ray photoelectron spectroscopic measurements of these surfaces show no difference in surface coverage, within experimental error, with $\theta = 40 \pm 20\%$,[19] indicating that steric factors such as the transition-state size or energy may have a significant role in determining the final surface packing density of such systems. The deep minima in ΔG_S for the phenyl-terminated surfaces at $\theta = 50\%$ correspond well with the experimental data for phenyl-functionalized surfaces prepared using the two-step halogenation/alkylation approach.[19]

While the data presented herein represent the thermodynamic parameters that govern the total percent alkylation of the surface, kinetics effects for real systems can potentially lead to a divergence from these predicted values. Previous studies[19] have shown that the electrochemical potential of the organometallic reagents used is sufficient to electrolytically cleave the Si−Cl bond, allowing the reaction to proceed through either a concerted mechanism or through a two-step dissociation/bond-formation process. The nature and size of transition states for each alkyl group being bonded to the surface, as well as the thermodynamic driving forces, will contribute significantly to the final packing density. The elevated temperatures (110°−120 °C) under which these reactions have been performed will favor the final alkyl packing densities approaching the thermodynamic packing densities predicted herein.

IV. Conclusions

Quantum mechanical calculations of the strain energies of bonded alkyl groups on the Si(111) surface, as well as of free energies for a collection of possible reaction pathways for the formation of Si−H bonds, have resulted in a framework for evaluation of the composition and structure of alkylated Si-(111) surfaces formed by the two-step chlorination/alkylation reaction. The reaction presumably starts with every atop site reacting to form either a Si−H bond or a Si−C bond. The competing termination reactions for each site are driven by both the thermodynamic energy as well as by various kinetics and steric considerations. The predicted free energy curves for the alkylation of the Si(111) surface most closely correspond with published data on the packing of these alkylated surfaces for ΔG_H values (formation energies for the reaction Si−H → Si−Cl in the presence of Grignard reagents in THF solvent) $\gtrsim -31$ kcal/mol. This is in accord with expectations for a reaction mechanism for the H-termination of unalkylated surface Si sites that involves the elimination of 2 H atoms and the formation of a C=C double bond in either unreacted Grignard R groups or in the THF solvent.

Acknowledgment. E.J.N. and N.S.L. gratefully acknowledge the NSF, Grant CHE-021358, for support of this work. S.D.S. and W.A.G. thank the Microelectronics Advanced Research Corporation (MARCO) and its Focus Center on NanoEngineered Architectonics (FENA).

Supporting Information Available: Pseudopotentials and basis sets; K-points and wave function grid settings. This material is available free of charge via the Internet at http://pubs.acs.org.

References and Notes

(1) Linford, M. R.; Chidsey, C. E. D. *J. Am. Chem. Soc.* **1993**, *115*, 12631−12632.
(2) Linford, M. R.; Fenter, P.; Eisenberger, P. M.; Chidsey, C. E. D. *J. Am. Chem. Soc.* **1995**, *117*, 3145−3155.
(3) Terry, J.; Linford, M. R.; Wigren, C.; Cao, R. Y.; Pianetta, P.; Chidsey, C. E. D. *Appl. Phys. Lett.* **1997**, *71*, 1056−1058.
(4) Terry, J.; Mo, R.; Wigren, C.; Cao, R. Y.; Mount, G.; Pianetta, P.; Linford, M. R.; Chidsey, C. E. D. *Nucl. Instrum. Methods B* **1997**, *133*, 94−101.
(5) Effenberger, F.; Gotz, G.; Bidlingmaier, B.; Wezstein, M. *Angew. Chem., Int. Ed.* **1998**, *37*, 2462−2464.
(6) Stewart, M. P.; Buriak, J. M. *Angew. Chem., Int. Ed.* **1998**, *23*, 3257.
(7) Sieval, A. B.; Demirel, A. L.; Nissink, J. W. M.; Linford, M. R.; van der Maas, J. H.; de Jeu, W. H.; Zuilhof, H.; Sudholter, E. J. R. *Langmuir* **1998**, *14*, 1759−1768.
(8) Sung, M. M.; Kluth, G. J.; Yauw, O. W.; Maboudian, R. *Langmuir* **1997**, *13*, 6164−6168.
(9) Zazzera, L. A.; Evans, J. F.; Deruelle, M.; Tirrell, M.; Kessel, C. R.; Mckeown, P. *J. Electrochem.* Soc. **1997**, *144*, 2184−2189.
(10) Buriak, J. M.; Allen, M. J. *J. Am. Chem. Soc.* **1998**, *120*, 1339−1340.
(11) Buriak, J. M.; Allen, M. J. *J. Lumin.* **1998**, *80*, 29−35.
(12) Holland, J. M.; Stewart, M. P.; Allen, M. J.; Buriak, J. M. *J. Solid State Chem.* **1999**, *147*, 251−258.
(13) Henry de Villeneuve, C.; Pinson, J.; Ozanam, F.; Chazalviel, J. N.; Allongue, P. In *Materials Research Society Symposium Proceedings*; 1997; Vol. 451, pp 185−195.
(14) Vieillard, C.; Warntjes, M.; Ozanam, F.; Chazalviel, J.-N. *Proc. Electrochem. Soc.* **1996**, *95*, 250.
(15) Bansal, A.; Li, X.; Lauermann, I.; Lewis, N. S.; Yi, S. I.; Weinberg, W. H. *J. Am. Chem. Soc.* **1996**, *118*, 7225−7226.
(16) Juang, A.; Scherman, O. A.; Grubbs, R. H.; Lewis, N. S. *Langmuir* **2001**, *17*, 1321−1323.
(17) Royea, W. J.; Juang, A.; Lewis, N. S. *Appl. Phys. Lett.* **2000**, *77*, 1988−1990.
(18) Webb, L. J.; Nemanick, E. J.; Biteen, J. S.; Knapp, D. W.; Michalak, D. J.; Traub, M. C.; Chan, A. S. Y.; Brunschwig, B. S.; Lewis, N. S. *J. Phys. Chem. B* **2005**, *109*, 3930−3937.
(19) Nemanick, E. J.; Hurley, P. T.; Brunschwig, B. S.; Lewis, N. S. *J. Phys. Chem. B* **2006**, in press.
(20) Webb, L. J.; Michalak, D. J.; Biteen, J. S.; Brunschwig, B. S.; Chan, A. S. Y.; Knapp, D. W.; Meyer, H. M.; Nemanick, E. J.; Traub, M. C.; Lewis, N. S. *J. Phys. Chem. B* **2006**, in press.
(21) Yu, H. B.; Webb, L. J.; Ries, R. S.; Solares, S. D.; Goddard, W. A.; Heath, J. R.; Lewis, N. S. *J. Phys. Chem. B* **2005**, *109*, 671−674.
(22) Yu, H. B.; Webb, L. J.; Solares, S. D.; Cao, P.; Goddard, W. A., III; Heath, J. R.; Lewis, N. S. *J.* Phys. Chem. B **2006**. Submitted for publication.
(23) Miyadera, T.; Koma, A.; Shimada, T. *Surf. Sci.* **2003**, *526*, 177−183.
(24) Hurley, P. T.; Nemanick, E. J.; Lewis, N. S. To be submitted.
(25) Sieval, A. B.; van der Hout, B.; Zuilhof, H.; Sudholter, E. J. R. *Langmuir* **2000**, *16*, 2987.
(26) Sieval, A. B.; van der Hout, B.; Zuilhof, H.; Sudholter, E. J. R. *Langmuir* **2001**, *17*, 2172−2181.
(27) Yuan, S.-L.; Cai, Z.-T.; Jiang, Y.-S. *New J. Chem.* **2003**, *27*, 626.
(28) Zhang, L.; Wesley, K.; Jiang, S. *Langmuir* **2001**, *17*, 6275.
(29) Shapiro, I. R.; Solares, S. D.; Esplandiu, M. J.; Wade, L. A.; Goddard, W. A., III; Collier, C. P. *J. Phys. Chem. B* **2004**, *108*, 13613−13618.
(30) Solares, S. D.; Esplandiu, M. J.; Goddard, W. A., III; Collier, C. P. *J. Phys. Chem. B* **2005**, *109*, 11493−11500.
(31) Mayo, S. L.; Olafson, B. D.; Goddard, W. A., III. *J. Phys. Chem. B* **1990**, *94*, 8897−8909.
(32) Rappé, A. K.; Goddard, W. A., III. *J. Phys. Chem. B* **1991**, *95*, 3358.
(33) Schultz, P. A. SeqQuest Electronic Structure; Sandia National Labs: Albuquerque, NM, http://dft.sandia.gov/Quest/.
(34) Perdew, J. P.; Burke, K.; Ernzerhof, M. *Phys. Rev. Lett.* **1996**, *77*, 3865.
(35) Solares, S. D.; Dasgupta, S.; Schultz, P. A.; Kim, Y. H.; Musgrave, C. B. and Goddard, W. A., III. *Langmuir* **2005,** *21*, 12404.